Patient-centered design method for self-powered and cost-optimized health monitors

MOLLY SHARONE[1], (Member, IEEE), AND ALI MUHTAROGLU[2,3], (Senior Member IEEE)
[1]Climate Technology Center & Network, UN Environment Programme, P.O. Box 30030, Gigiri-Nairobi, Kenya
[2]Department of Mechanical, Electronic and Chemical Engineering (MEK), Oslo Metropolitan University – OsloMet, 0130 Oslo, Norway
[3] Advanced Health Intelligence and Brain-Inspired Technologies (ADEPT) Research Group, OsloMet, 0130 Oslo, Norway

Corresponding author: Ali Muhtaroglu (alimuhta@oslomet.no).

ABSTRACT The emergence of Wireless Body Area Networks (WBANs) with health monitoring capabilities has revolutionized health care. Implementing fully independent WBAN nodes is important to the long-term viability of this initiative. Regularly recharged and depletable batteries remain a significant impediment in such systems. Energy harvesting (EH) from environmentally clean sources has thus been receiving increasing attention. Nevertheless, the autonomy and optimization of existing WBAN sensor nodes have remained questionable because methods that integrate realistic usage conditions into the design process have been lacking. A plausible method is proposed to establish a framework for designing a sustainable health monitoring node in this work. A Health Monitoring Energy System (HeMeS) tool prototype is consequently developed using comprehensive analytical models and utilized to demonstrate system design space exploration for various patient types, incorporating environmental factors, electronic load activity levels, and system cost/size constraints. It is concluded that the patient-centered system design approach incorporating interactions across transducers, electronics, sensors, user environment and data duty-cycling profiles, is viable, and is in fact appealing in safeguarding truly autonomous and cost-optimal WBANs that are compatible with climate-neutral society.

INDEX TERMS Self-powered, cost effective, energy harvesting, health monitoring, system models.

I. INTRODUCTION

The UN's Sustainable Development Goal 13 is focused on taking urgent action to combat climate change and its impact. A zero-carbon economy is also one of the EU's 2050 goals [1]. Self-powered operation is required of personal health monitoring systems as such assistive mobile platforms find broad utilization in exponentially increasing number of machine-to-machine interfaces. Energy autonomy not only prevents WBAN operations from being disrupted, but it also eliminates the need to replace batteries on a regular basis [2]. Energy harvesting (EH) is fundamental for fully autonomous WBANs, as it involves transforming energy from ambient sources that would be wasted, into useful electrical energy [3]-[6]. Attaining complete autonomy in WBANs has become feasible because of miniaturized ultra-low-power WBANs, system design techniques including transmission schedules and efficient resource allocation [7].

The design and modeling of interface electronics for Energy Harvesters were the focus of [8] and [9]. A power management unit that uses either PV cells or TEG to power a biological load was presented in [10]. To maximize the lifetime in EH for wireless body sensor networks, Badri et al. [11] focused on dynamic slot allocation at distinct sensor nodes (WSN). Fan et al. [12] used data from diverse human activities and environmental variables to examine available power from EH. Transmission scheduling in wearable health monitoring systems was proposed by Guo et al. [13] to optimize energy utilization from the harvester to the loads. In [14] an autonomous WBAN node for health monitoring was powered using solar energy. Such systems are suitable for non-critical patients but is impractical for hospitalized patients with minimal to no mobility, or outdoor exposure. Dionisi et al. [25] developed a batteryless, self-sustained wearable system for measuring heart rate, torso movement and respiration rate. Centered around measured vitals, the system is not based on diversified activity and environmental conditions of the patients. The patient is required to spend a certain amount of time in a well-lit environment to obtain solar energy before the system becomes obsolete.

While these studies are crucial in demonstrating the feasibility of self-powered health monitoring systems under a set of assumptions, it is important to have tools and methods to address the energy flow optimization in any self-powered health monitoring system. In [26], Tobola et al. developed an Ultra-Low Power Sensor Evaluation Kit (ULPSEK) for designing modulated, ultra-low power sensors, to be used together with a web-based battery runtime calculator. In [15], Tobola demonstrated that ULPSEK could be powered through harvested body heat using a thermoelectric (TE) harvester

with an average output power of 171 µW. Such studies are important towards understanding the power flow in autonomous self-sustained health monitoring devices. However, such tools fall short for exploration in the early design stages. In addition, consideration of the patient type and environment is lacking, missing system optimization opportunities. Lack of consistent design methods and tool flows inevitably results in overdesign of some systems, which potentially increases cost, size, and materials. In other cases, the question of autonomy and conditions under which autonomy applies, remain open. The interactions across the components of a system need to be studied on one hand, to optimize an energy autonomous WBAN for performance, size, and cost. On the other hand, incorporating realistic usage scenarios ensure power generation, losses, delivery, and consumption are adequately and accurately accounted for. Practical solutions require cross-disciplinary outreach to the environment of the patients, as depicted in Fig. 1. In addition, a new set of tools are needed to enable an exhaustive cognizance of various design trade-offs.

This paper proposes a method for sustainable, cost-effective custom design of an autonomous health monitoring node by positioning the patient environment to the center of the system design. Section II outlines the main categories of patients to be health monitored. The proposed health monitoring system design method and associated tool architecture are described in Section III. Section IV reviews the implementation of a tool prototype, HeMeS, based on analytical modeling that is consistent with the proposed methodology framework. Using HeMeS for exploring the system design space, variations in the design of autonomous WBAN nodes are demonstrated through an example in Section V for different categories of patients. Finally, Section VI summarizes the conclusions from this work.
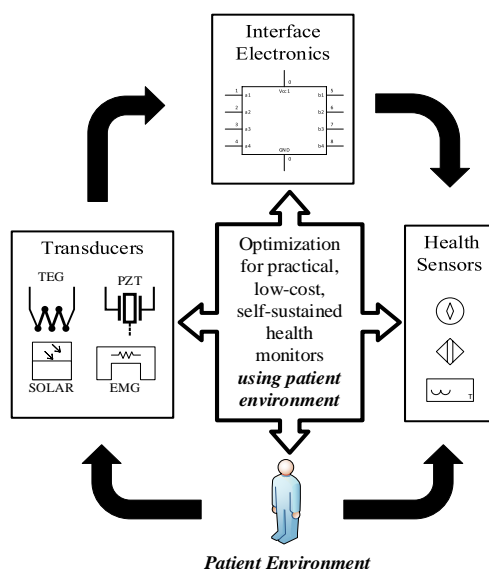

FIGURE 1. Opportunity for optimized fully autonomous health monitoring sensors through integration of patient environment into the system design flow.

II. TARGET ENVIRONMENT

Patients vary in their environment and their physical capabilities. It follows that the health monitoring devices used by each patient should be customized to sustainably cater for the needs of different categories of patients and to allow for sufficient energy to be harvested based on patients' activity profile and environment. Background is provided here on three primary patient types targeted for this work.

Non-critical patient: A non-critical patient is relatively mobile and uses a WBAN node to continuously monitor bio-signals for early detection of anomalies. Demand for such monitors has recently increased to counter the fast increasing health care costs [3]. Patients in this category can be very active during jogging exercises with reasonable power generation potential from vibration-based sources such as piezoelectric (PZT) transducers [17].

Nursing home patient: According to Georgie and Jeannes [18], older adults living in nursing homes require monitoring of vitals due to chronic conditions such as heart disease and diabetes [18] or for early detection of any abnormal events such as falling [19]. Physical activity is significantly reduced in this patient category. In addition, these patients are more prone to posthospital syndrome, which is the likelihood of the elderly being readmitted to the hospital after an initial visit due to their frail nature [20]. It follows that the vibrations from their motion occur at lower frequencies with less opportunity for power generation from vibration-based sources compared to the environment of younger people or non-critical patients.

Hospitalized patient: WBANs can be used to monitor hospitalized patients to enable early ambulation and to monitor patient deterioration in wards [21]. A hospitalized patient in this case can be defined as one that is bedridden and in no position to move. Therefore, the design space exploration of this patient will mainly be influenced by the amount of harvestable thermal body power.

It is crucial to explore the design space with a target application and evaluate the performance of self-sustained WBAN nodes accordingly. The use of the above profiles to derive indicative physical environmental parameters for energy harvesting as well as specification of electronic loads as part of a customized system design methodology is further explored in the next section.

III. METHOD AND SYSTEM ARCHITECTURE

It is possible to design self-sustained (self-powered without charging requirement) health monitoring systems with state-of-the-art hybrid energy harvesting sources, highly efficient interface circuits, energy-aware sensors, and power management techniques. When the generated energy is insufficient to sustain the desired sensor load, larger and more capable energy harvesters with higher output power capacity can be considered at higher material and design costs. Therefore, the design optimization task needs to incorporate patient environment to avoid under- or over-design.
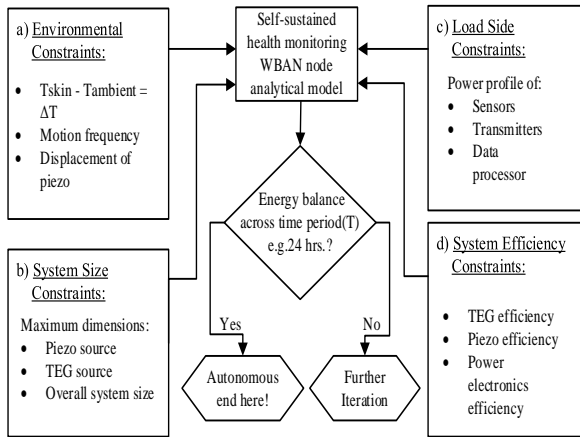
FIGURE 2. Patient-centered design method for self-sustained health monitoring WBAN node.

A. Methodology

Fig. 2 depicts the integration of relevant constraints into an iterative method that comprises of:

(a) Environmental constraints: These are the constraints that represent the environment and condition of the patient and are used to derive fundamental power generation input parameters. For a system powered by hybrid thermal-vibrational energy harvesting, the average temperature difference between the skin and the ambient air as well as displacement and vibration frequency of the PZT mass are critical.

(b) Load side constraints: Such constraints consist of desired sensors for health monitoring, the communication channel between the WBAN node and base station, processor, and associated power consumption profile for each of these components that incorporates power management features, including transmission and sleep/wake-up schedule.

(c) System size constraints: System size is mainly influenced by the collection of components and overall packaging on an electronic board. As the number of features increase, the system size (and cost) may grow prohibitively large for on-skin, under-skin, or generally wearable applications.

FIGURE3. HeMeS core model with hybrid harvesting example block diagram.

(d) System efficiency constraints: Continual improvements in design and material technologies of transducers, electronics, and sensors result in efficiency benefits, which directly reduce energy losses and improve average power dissipation. Tracking of these constraints is essential to integrate associated benefits.

Analytical modeling is utilized to consolidate all constraints into an iterative energy balancing tool, which completes an energy sweep across 24 hours to check for system autonomy under varying environmental, system size, load side, and system efficiency constraints, as demonstrated in Fig. 2. If and when the system autonomy is established by the tool, then the optimization iterations end for a given patient environment, and the system can move to implementation with high confidence. Longevity and scalability of health monitoring systems typically improve with technological advancements over time, which can directly be reflected to the constraint parameters for projections and what-if studies.

B. Tool System Architecture

The architecture of the first tool prototype, named HeMeS (Health Monitoring Energy System), is presented in Fig. 3. The sources are interfaced with converters for power conditioning, an energy storage buffer, a regulator to maintain a constant voltage to the loads, and the loads used in health monitoring. The loads comprise of health monitoring sensors, a processor, a transceiver, and a display.

IV. HEMES TOOL PROTOTYPE MODEL

The development of analytical features in HeMeS is followed by MATLAB/Simulink modeling using a hierarchical design approach. The prototype includes two power generation sources based on thermal-vibrational energy harvesting, a storage device, and a load that represents a collection of electronic components in a WBAN node. A brief description of each system component is provided in the following sections.

A. Piezoelectric Energy Harvester

A PZT energy harvesting transducer converts vibrations to electricity through direct piezoelectric effect [25]. The detailed derivation of the induced charge by a piezo bender can be found in [26] and is not repeated here as it is not the focus of this work. Instead, the PZT harvester is modelled based on a piezo bender from the Simscape library in MATLAB whose boundary conditions are as follows:

The left end of the piezo bender is clamped to the human body (as HeMeS tool can be used in diverse forms, the location of the piezo bender is not limited to one specific area but can be customized depending on the use case), forcing the motion. The right end of the piezo bender is connected to an extra mass. Due to the elasticity, mass, and inertia of the piezo bender, the motion of the right end is not synchronous to the left end. The deformations produce then a charge and voltage across the electrical terminals of the piezo bender, that are harvested into power. It must be noted that, this
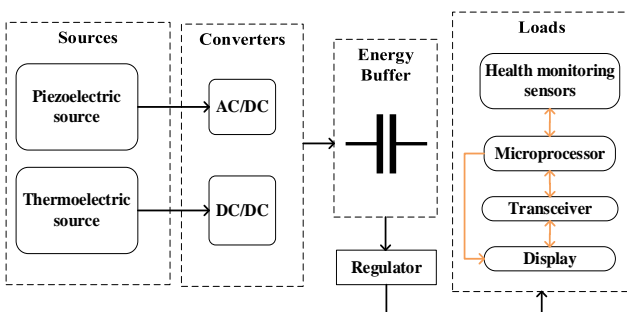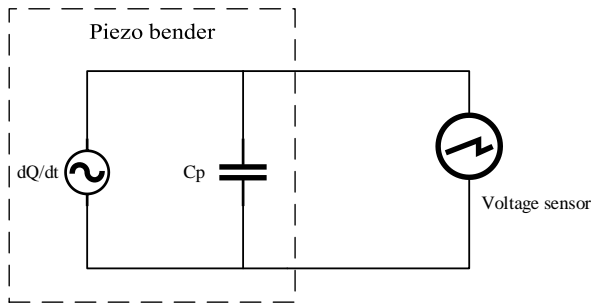
FIGURE 4. Induced voltage from the piezo model.

clamped piezo bender has both displacement and rotation equal to zero [27]. The commercial piezo bender T220-H4BR-1305XB, is chosen as the default PZT generator due to its desirable properties such as size and material flexibility for WBAN application. TABLE I presents specifications used to calculate the fundamental material parameters (Piezoelectric stress coefficient(e_{31}), Young's Modulus(E), Dielectric constant(ε), and the resonance frequency(f_0)) of the piezo generator (1-3) as:

$$e_{31} = \frac{2\,l\,F_{block}}{3\,d\,w\,V_{rated}}, \tag{1}$$

$$E = -\frac{4\,F_{block}\,l^3}{y_{free}d^3\,w}, \tag{2}$$

$$\varepsilon = \frac{d}{lw}\left(C_{piezo} + \frac{4\,F_{block}\,y_{free}}{V_{rated}^2}\right). \tag{3}$$

Equation (4) is used to calculate the first resonance frequency(f_0) of the piezo bender as shown below.

$$2\pi f_0 = 1.855^2\sqrt{\frac{EI}{m\,l^3}}. \tag{4}$$

The calculated fundamental material parameters are thereupon summarized in TABLE II. Voltage output of the piezo bender can be sensed, as depicted in Fig. 4, based on the amount of charge accumulated across the electrodes. Current flowing through the PZT capacitor can also be calculated as in (5) [29]:

TABLE I
DATASHEET PARAMETERS FOR T220-H4BR-1305XB [28]

Parameter	Value
Thickness (d)	0.51 mm
Width (w)	12.7 mm
Length (l)	31.7 mm
Mass (m)	1.6 g
Free deflection at rated voltage (y_{free})	0.25 mm
Rated Voltage (V_{rated})	60 V
Capacitance (C_{piezo})	24 nF
Blocking force at rated voltage (F_{block})	0.28 N

TABLE II
CALCULATED FUNDAMENTAL MATERIAL PARAMETERS

Fundamental Parameter	Calculated Value
Dielectric constant (ε)	1.28932×10^{-7} F/m
Young's Modulus (E)	8.5514×10^{10} N/m^2
PZT stress coefficient (e_{31})	15.275 C/m^2
First resonance frequency (f_0)	52.8 Hz

TABLE III
PARAMETERS FOR MODELING TEG IN MATLAB / SIMULINK [31],[32]

Description	Symbol	Value
Temperature of the body	T_{body}	310 K
Seebeck coefficient of P-type leg	α_p	186e-6 V/K
Seebeck coefficient of n-type leg	α_n	-186e-6 V/K
No. of leg pairs	N	199
Skin's thermal resistance	φ_{skin}	3.218 K/W
Heat sink's thermal resistance	$\varphi_{heatSINK}$	21.74 K/W
Ratio of Rload: R_{TEG}	x	1

$$I_p = C_p\frac{dV_p}{dt}. \tag{5}$$

Consequently, the PZT harvester power generation under proper rectification conditions can be determined in the form:

$$P_{in} = V_pI_p. \tag{6}$$

B. Thermoelectric Energy Harvester

A thermoelectric harvester employs Seebeck effect to produce electricity from a thermopile by converting temperature gradients to electric power [30], [31]. Heat flow from the hot to cold junctions for thermal energy harvesting is expressed using (7a-b):

$$\frac{T_{body}-T_h}{\phi_{skin}} = K(T_h-T_c)+SIT_h-0.5I^2R = Q_h, \tag{7a}$$

$$\frac{T_c-T_{air}}{\phi_{heatSINK}} = K(T_h-T_c)+SIT_c+0.5I^2R = Q_c, \tag{7b}$$

where T_{body} and T_{air} are the temperature of the body and ambient temperature, Φ_{skin} and $\Phi_{heatSINK}$ are thermal resistance of the skin and thermal resistance of the heat sink, and finally $S, K, R,$ are Seebeck coefficient of the module, thermal conductance of the module, and the electrical resistivity of the module, respectively. Pietrzyk *et al.*'s model in [31] includes the losses such as Peltier effect, Joule heating, and thermal resistances at each junction, and has thus, been used to construct the TE model in HeMeS. (7a-b) can be solved iteratively utilizing datasheet parameters listed in TABLE III to determine the actual temperature of the hot and cold sides of the TEG.

The thermoelectric generator's induced voltage and power are estimated in MATLAB using Th and Tc values (8-9) [32]:

$$V = \frac{(S(T_h-T_c))x}{x+1}, \tag{8}$$

$$P = IV = \frac{(S(T_h-T_c))^2x}{R(x+1)^2}. \tag{9}$$

C. Interface Electronics

WBAN loads, such as sensors, processors, communication modules, are predominantly powered using DC voltage [5]. PZT harvester's AC voltage must be rectified and stepped down using a buck converter. Conversely, the TE harvester's low DC voltage output must be stepped up to the required amount for charge storage. Both boost and buck converters used in the HeMeS tool are modeled with associated power

4

conversion efficiency parameter, as illustrated in (10) [32]:

$$I_{out\_converter} = \frac{\eta \cdot P_{harvester}}{V_{SC}}, \tag{10}$$

where $I_{out\_converter}$, $P_{harvester}$, η, and V_{SC} are converter output current, harvester output power, converter efficiency, and storage capacitor voltage (converter output voltage), respectively. The converter efficiency parameter accounts for the conversion losses.

Simulink blocks are used to mimic the rectifier and a filter to eliminate voltage ripple in the PZT harvester. The LTC-3588 harvester IC, which includes a bridge rectifier, a filter and a high-efficiency buck converter is modeled to attain the complete model of the PZT harvester shown in Fig. 5.

Because both PZT and TEG sources are designed to be available simultaneously, small TEG voltage is boosted to the same level as the piezoelectric voltage (3.3V). TI-BQ25504 harvester IC is modeled to simulate the TEG DC/DC converter, with the associated efficiency parameter.

The full configuration for the TEG is shown in Fig. 6.

D. Storage Unit (Energy Buffer)

TEG and PZT sources charge an intermediate storage unit, such as a supercapacitor, which in turn powers the health monitoring system load. Fig. 7 depicts an equivalent circuit, used to derive the equations (11-14):

$$V_{sc} = V_c + V_{ESR}, \tag{11}$$

$$V_C = \frac{1}{C} \int I_C(t)\, dt + V_{c0}, \tag{12}$$

$$V_{ESR} = I_{charge} \cdot ESR, \tag{13}$$

$$I_C = I_{charge} - I_{leak} - I_{discharge}, \tag{14}$$

where V_{sc}, V_c, ESR, and I_c are supercapacitor effective voltage including the drop across series resistance, capacitor voltage, electrical series resistance, and capacitor current respectively. Commercial PB-5R0V104-R 100 mF supercapacitor from Eaton was chosen in this application. Its datasheet is used to obtain the values of the equivalent series resistance (ESR), leakage current, and the rated capacitance [36].

E. Loads

The storage is discharged due to the average total current consumption at the loads. HeMeS facilitates the computation of total average current by allowing users to enter different activity levels and estimated activity intervals for each load device. The parameters are compatible with power management practices such as transmission scheduling. Loads are only active based on entered on/off activity factors, and energy is only dissipated when collected in sufficient amount at the storage unit. Any gaps in the average accumulated versus consumed charge is flagged by the tool. TABLE IV outlines sample load parameter values used in HeMeS analysis. Power consumption at each activity level is determined from representative datasheets for each component at the regulated voltage.
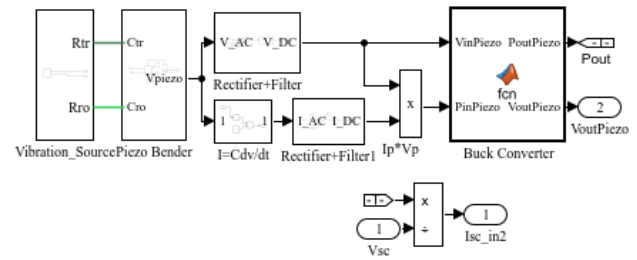

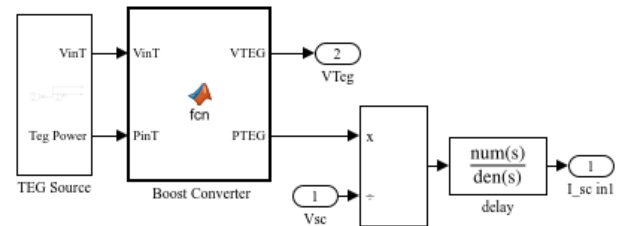**FIGURE 5.** Configuration of the PZT harvester and interface electronics in Simulink.

FIGURE 6. Configuration of the TEG harvester and interface electronics in Simulink.

V. DESIGN SPACE EXPLORATION

For a monitored patient with a repeating activity profile, the minimum required period for balancing the energy in the WBAN node is set as T=24 hours, which is a configurable parameter. As various parameters in any of the four peripheral constraint boxes previously presented in Fig. 2 change, the possibility of convergence to a new autonomous design can be investigated. The average values in Table V
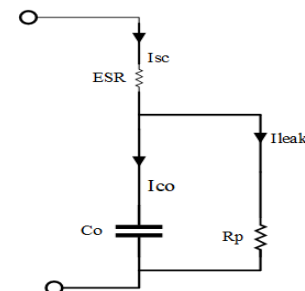

FIGURE 7. Equivalent circuit of a supercapacitor [34].

TABLE IV
DEFAULT LOAD (% TIME IN STATE VALUES VARY WITH PATIENT PROFILE)

Load Component	Power State	Power Dissipation	% Time in State
Processor	Active, Idle	$10 - 100\ \mu W$ $1.5\ \mu W$	5% 95%
Low Power Bluetooth	Active, Idle	4 mW $1\ \mu W$	4% 96%
Temperature Sensor	Active	$10\ \mu W$	100%
Accelerometer	Active	$60\ \mu W$	100%
Pulse Rate Sensor	Active, Idle	$200\ \mu W$ $2\ \mu W$	10% 90%
ECG Sensor	Active, Idle	6 mW 25 nW	3% 97%

TABLE V

DERIVATION OF INDICATIVE PHYSICAL ENVIRONMENTAL PARAMETERS FOR ACCURATE PREDICTION OF POTENTIAL ENERGY AVAILABLE FOR HEALTH MONITORS

	Non-critical	Nursing home	Hospitalized
Living space profile	Room temperature (approx. 25°C)	Room temperature (approx. 25°C)	Temperature regulated according to treatment
Activity profile	Jogging, Working, Sleeping	Low intensity workouts, Resting sessions, Sleeping	Minimal Activity

	Conversion to typical energy harvesting opportunity averaged over 24hrs		
	Non-critical	Nursing home	Hospitalized
ΔT	Body temperature minus living space temperature (Tbody-Tambient)		
Vibration frequency	4Hz	2Hz	Minimal to no vibration

show the daily activity profile of both young individuals and senior patients, as well as the corresponding frequency of human motion in [39], based on hourly data from the literature [37], [38]. Environmental (ambient temperature) restrictions for older patients are also integrated [40]. The recommended activity levels are calculated using the guidelines in [41]. For size/cost optimization, the initial system size (before iterations) is initially aimed at around 10 cm^3. Minimum patient activity, environmental conditions, maximum load activity, and minimum system size are all variables that can be targeted in the analysis, with the remaining system characteristics fixed for this exercise, including power generation, power conversion and energy storage components summarized in TABLE VI. One intermediate output of the tool is average ΔT and motion frequency parameters over a period of T, as depicted in Table VII, which directly impact the power generation capacity in the system.

The analyses that follow will be iterated by turning a frequency-up-conversion (FUC) design option for vibrational energy harvesting ON and OFF, to demonstrate design space exploration. FUC feature allows a mechanical spring module to be integrated into the system package to convert low movement frequencies to higher frequencies and thus achieve higher power generation from PZT transducers with resonance profiles that include higher frequencies.

A. Load Activity Constrained Analysis to Determine Minimum Patient Activity and Environmental Factors

Given the default settings (Tables IV, VI) and a 10 cm^3 overall system size constraint, the minimum patient activity set (PZT generation) and minimum temperature gradient set (TE generation) are determined for autonomous operation in each patient category. The parameter sweep range was kept narrow for minimum deviation from common profiles in the literature to arrive at a solution, because the optimal answer for patient activity can only be identified in collaboration with a medical specialist (which is part of future plans). One

way to interpret a solution with minimum patient activity and least constraining environmental factors is that this solution provides the best opportunity in cost-optimizing the autonomous operation of the health monitoring WBAN. Depending on the level of strain, non-critical patients can be physically active with a PZT frequency of up to 4 Hz [17]. For self-sustained health monitoring with the FUC option selected, the minimum average frequency of motion per day should be 1.27 Hz, and the average ambient temperature over 24 hours should not exceed 22.7 °C. Without the FUC option, the average temperature gradient must increase by 0.66 °C, as well as increased physical activity, for adequate power to be produced in the autonomous system. Nursing home residents are less active as they get older. When the FUC is activated, an autonomous WBAN node should have a minimum average of 1 Hz, as well as a minimum temperature gradient of 14.52 °C. When FUC is disabled, the average increase in activity is 0.54 Hz, and the average rise in temperature gradient is 0.48 °C. Because the TEG is virtually the only source of power in the case of hospitalized patient, the system should not invest in a FUC functionality in this situation. For the system to operate autonomously without movement for 24 hours, a minimum average temperature gradient of 15.02 °C is required.

Fig. 8 depicts the influence of FUC integration on minimum attained patient activity and temperature gradient across the selected 24-hour period for energy balancing in each patient category. Disabling the FUC option to minimize system cost and/or volume, results in additional restraints on the patient environment, as depicted by the red zones in the figure.

B. User Activity Constrained Analysis to Determine Maximum Health Monitoring Load Activity

Increased data processing and communications correspond to higher activity levels for system loads. In this case, load activity parameters are iterated with fixed system size, and patient environment (and activity).

A FUC-enabled system enables for more frequent sensing, processing, and communication for the WBAN node, as expected. This is due to the hybrid harvester's decreased power capacity without the FUC feature. The maximum permissible activity of loads over 24 hours for self-sustained operation is depicted in Fig. 9. Because the patient has little

TABLE VI
POWER GENERATION/CONVERSION, AND ENERGY STORAGE COMPONENTS

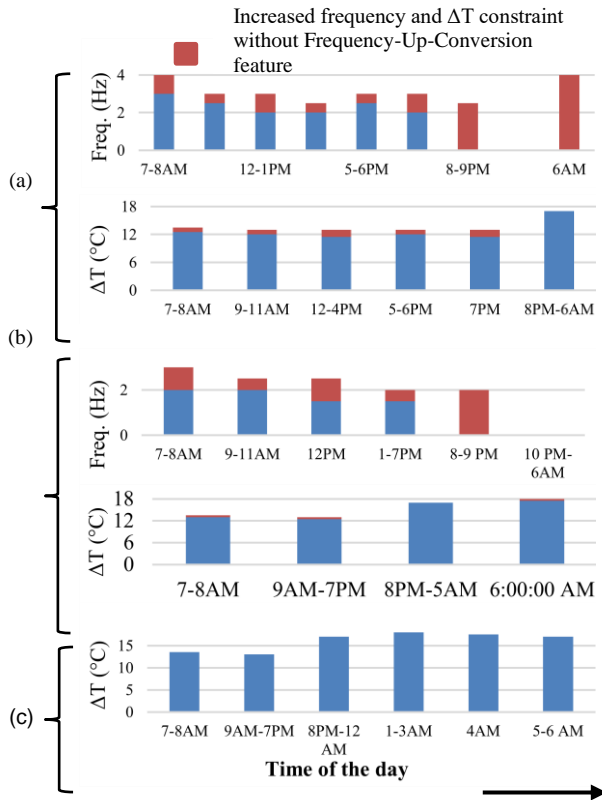| Component	Origin	Model
Piezo source	T220-H4BR-1305XB	MIDE
TEG source	TEG2-126LDT	TEC
Boost converter	BQ-25504 & TPS61070	Texas Instruments
Buck converter	LTC-3588	Linear Technology
Storage capacitor	PB-5R0V104-R	Eaton

FIGURE 8. 24-hour activity and environmental condition (ΔT) requirement for self-powered health monitoring with and without the FUC feature for (a) non-critical, (b) nursing home, and (c) hospitalized patient.
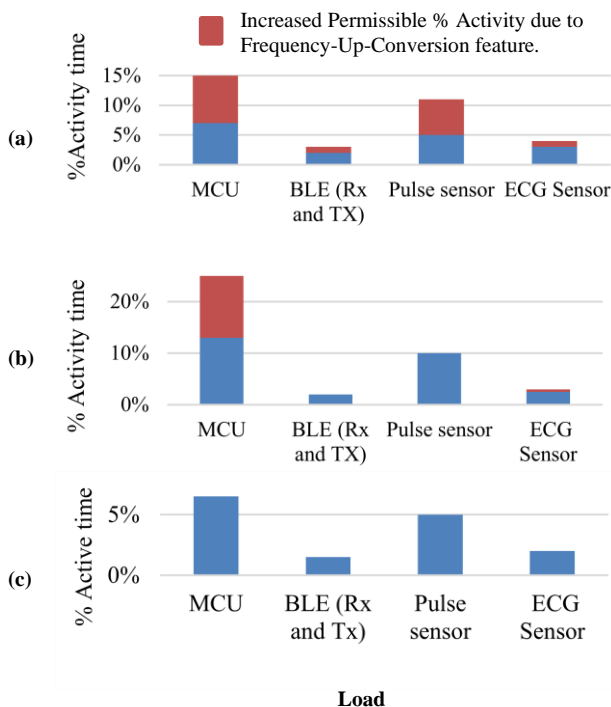

FIGURE 9. % load activity permissible with and without the FUC feature for (a) non-critical, (b) nursing home, and (c) hospitalized patient.

Patient Type	Avg ΔT	Avg. freq. of motion
Nursing home patient (e.g., elderly)	14.52 °C	1 Hz
Hospitalized patient	15.02 °C	-
Non- critical	14.21 °C	1.27 Hz

activity in the third patient scenario the permissible load activity is the same with and without the FUC.

VI. CONCLUSIONS AND FUTURE WORK

With present sustainability issues and aggressive zero-carbon goals, health sector cannot be left behind in efforts to move sensor nodes to self-powered mode with maximum savings in materials. In fact, if customized user-aware system optimizations can be implemented in the health sector, it can have a catalyzing effect on others. The efficacy of self-powered WBAN for health monitoring is significantly affected by the patient's environment and activity. This study shows a MATLAB prototype of an autonomous Health-Monitoring Energy System (HeMeS) tool that uses the proposed methodology for designing self-sustaining and cost-optimized health monitors. Component analytical models, sensitive physical and environmental factors, load specifications, and patient activity information are all combined for unified electrical modeling of energy flow in an autonomous WBAN node.

Table VIII summarizes the changes in given variables for design space exploration under different constraints. It is worth noting that when there is no FUC in the system, a higher temperature gradient is required to harvest enough energy for autonomous operation. This results in the requirement of a temperature-regulated environment, which can be costly, and illustrates the importance of hybridized harvesting solutions where the patient can benefit from other ambient sources such as vibration from movement. Minimum patient activity and environmental conditions, maximum allowed load activity, and minimum system size (last row in Table VIII) were evaluated with and without the Frequency-Up-Conversion feature. The presented methods and tools can also be used to investigate various design trade-offs for self-sustaining health monitoring devices, such as the viability of alternate hybrid generation modes, new MEMS transducer applications, more efficient circuits, and new power management strategies. As a result, autonomous health monitoring solutions that are both cost-effective and space-saving are possible.

The results of this research demonstrated that ultimate system optimization in self-powered sensors requires integration of application data, in this case, patient. be used in multi-disciplinary studies to co-design sensor nodes and energy harvester modules to properly anticipate energy flows and advise design decisions based on the environment

TABLE VIII
COST OPTIMIZATION TABLE

Constrained Parameter	Variable Parameter	Non-critical			Nursing Home			Hospitalized
		FUC enabled	FUC disabled	% Change in variable constraint	FUC enabled	FUC disabled	% Change in variable constraint	No movement
Load activity, system size	Frequency of movement	1.27 Hz	2.04 Hz	60% ⬆	1 Hz	1.54 Hz	54% ⬆	-
	Temperature gradient	14.21 °C	14.87 °C	4.64% ⬆	14.52 °C	15 °C	3.30% ⬆	15.02 °C
Patient movement, system size	MCU active time	15%	7%	53% ⬇	25%	13%	48% ⬇	6%
	BLE active time	3%	2%	33.30% ⬇	2%	2%	0%	1.50%
	ECG sensor active time	4%	3%	25% ⬇	3%	2.50%	16.70% ⬇	2%
	Pulse rate sensor active time	11%	5%	54% ⬇	10%	10%	0%	5%
Load activity, patient movement	System size	10 cm^3	12 cm^3	20% ⬆	10.4 cm^3	12 cm^3	15.40% ⬆	10 cm^3

and activity. Associated methods and tools can collective behavior of the components and applications that make up a self-powered wearable body area network. The concepts presented can be extended to future energy-autonomous sensor networks and robotics. Next steps include the exploration of the impacts on autonomy of the WBAN nodes, with changes in the location of the transducers from one part of the body to another. In addition, future work will investigate artificial intelligence for dynamic energy balancing and further system cost optimization.

REFERENCES

[1] European Commission, "A Clean Planet for all. A European long-term strategic vision for a prosperous, modern, competitive and climate neutral economy," *Com,* vol. 773, p. 114, November 2018, [Online]. Available: https://eur-lex.europa.eu/legal-content/EN/TXT/PDF/?uri=CELEX:52018DC0773 (accessed 4.11.2023).

[2] J. Selvarathinam and A. S. Anpalagan, "Energy harvesting from the human body for biomedical applications," no. December, pp. 6–12, 2016.

[3] S. M. Demir, F. Al-Turjman, and A. Muhtaroglu, "Energy Scavenging Methods for WBAN Applications: A Review," *IEEE Sens. J.*, vol. 18, no. 16, pp. 6477–6488, 2018.

[4] M. A. Wahba, A. S. Ashour, and R. Ghannam, "Prediction of harvestable energy for self-powered wearable healthcare devices: Filling a gap," *IEEE Access*, vol. 8, pp. 170336–170354, 2020.

[5] C. Lu, V. Raghunathan, and K. Roy, "Efficient design of micro-scale energy harvesting systems," *IEEE J. Emerg. Sel. Top. Circuits Syst.*, vol. 1, no. 3, pp. 254–266, 2011, doi: 10.1109/JETCAS.2011.2162161.

[6] S. A. Murawski, W. T. Hogarth, E. B. Peebles, and L. Barbeiri, "Prevalence of External Skin Lesions and Polycyclic Aromatic Hydrocarbon Concentrations in Gulf of Mexico Fishes, Post-Deepwater Horizon," *Trans. Am. Fish. Soc.*, vol. 143, no. 4, pp. 1084–1097, 2014.

[7] L. Mateu and F. Moll, "Review of energy harvesting techniques and applications for microelectronics," no. June 2005, 2021.

[8] M. Ben Ammar, "Design of a DC-DC Boost Converter of Hybrid Energy Harvester for Low-Power Biomedical Applications," pp. 955–959, 2020.

[9] Sayed Mohammad Noghabaei and Mohama Sawan, "A fully integrated High-Efficiency Step-up DC-DC converter fro energy Harvesting applications," pp. 121–122, 2016.

[10] A. Roy and B. H. Calhoun, "A 71 % Efficient Energy Harvesting and Power Management Unit for sub- ₃ W Power Biomedical Applications," pp. 1–4, 2017.

[11] N. Badri, L. Nasraoui, L. A. Saidane, and S. Ikki, "Maximizing Lifetime in Energy-Harvesting WBSN for Health Monitoring Systems Through Dynamic Slots Allocation," pp. 325–329, 2019.

[12] D. Fan, L. L. Ruiz, J. Gong, and J. Lach, "EHDC: An Energy Harvesting Modeling and Profiling Platform for Body Sensor Networks," vol. 22, no. 1, pp. 33–39, 2018.

[13] L. Guo, S. Member, Z. Chen, and D. Zhang, "Sustainability in Body Sensor Networks With Transmission Scheduling and Energy Harvesting," vol. 6, no. 6, pp. 9633–9644, 2019.

[14] T. Wu, F. Wu, J. M. Redoute, and M. R. Yuce, "An Autonomous Wireless Body Area Network Implementation Towards IoT Connected Healthcare Applications," *IEEE Access*, vol. 5, no. July, pp. 11413–11422, 2017.

[15] A. Tobola *et al.*, "Self-Powered Multiparameter Health Sensor," *IEEE J. Biomed. Heal. Informatics*, vol. 22, no. 1, pp. 15–22, 2018.

[16] E. Saoutieff *et al.*, "A wearable low-power sensing platform for environmental and health monitoring: The convergence project," *Sensors*, vol. 21, no. 5, pp. 1–21, 2021.

[17] M. A. Halim, H. O. Cho, and J. Y. Park, "A handy motion driven, frequency up-converting piezoelectric energy harvester using flexible base for wearable sensors applications," *2015 IEEE SENSORS - Proc.*, 2015.

[18] N. Georgi and R. Le Bouquin Jeannes, "Proposal of a remote monitoring system for elderly health prevention," *2017 Int. Conf. Smart, Monit. Control. Cities, SM2C 2017*, pp. 69–74, 2017.

[19] N. Stefanos, D. D. Vergados, and I. Anagnostopoulos, "Health care information systems and personalized services for assisting living of Elderly people at nursing home," *Proc. - 3rd Int. Work. Semant. Media Adapt. Pers. SMAP 2008*, pp. 122–127, 2008.

[20] V. Patel, A. Orchanian-cheff, and R. Wu, "Evaluating the Validity and Utility of Wearable Technology for Continuously Monitoring Patients in a Hospital Setting : Systematic Review," vol. 9, no. 8, 2021.

[21] M. Joshi *et al.*, "Wearable sensors to improve detection of patient deterioration," *Expert Rev. Med. Devices*, vol. 0, no. 0, p. 1, Feb. 2019.

[22] A. Khaligh, P. Zeng, X. Wu, and Y. Xu, "A hybrid energy scavenging topology for human-powered mobile electronics," *IECON Proc. (Industrial Electron. Conf.*, pp. 448–453, 2008.

[23] A. Dionisi, D. Marioli, E. Sardini, and M. Serpelloni, "Autonomous

Wearable System for Vital Signs Measurement With Energy-Harvesting Module," *IEEE Trans. Instrum. Meas.*, vol. 65, no. 6, pp. 1423–1434, 2016.

[24] A. Tobola *et al.*, "Battery Runtime Optimization Toolbox for Wearable Biomedical Sensors," pp. 199–204, 2016.

[25] E. B. Tadmor and G. Kosa, "Electromechanical coupling correction for piezoelectric layered beams," in Journal of Microelectromechanical Systems, vol. 12, no. 6, pp. 899-906, Dec. 2003, doi: 10.1109/JMEMS.2003.820286.

[26] Xiangyang Li, Deepesh Upadrashta, Kaiping Yu, Yaowen Yang, Analytical modeling and validation of multi-mode piezoelectric energy harvester, Mechanical Systems and Signal Processing, Volume 124,2019, Pages 613-631, ISSN 0888-3270, https://doi.org/10.1016/j.ymssp.2019.02.003.

[27] The MathWorks Inc. *Piezo Bender Documentation*. Piezoelectric bimorph beam of rectangular cross-section - MATLAB. https://www.mathworks.com/help/sps/ref/piezobender.html ,2021

[28] *PIEZO.COM Materials Technical Data*, MIDE, Woburn, MA, USA, 2020.

[29] T. Eggborn, "Analytical Models to Predict Power Harvesting with Piezoelectric Materials," *Masters Thesis, Virginia Polytech. Inst. State Univ. VA Frederick, A. A., Clark, W. W., Hu, H*, vol. 5, no. May, p. 11, 2003.

[30] E. Kanimba and Z. Tian, "Modeling of a Thermoelectric Generator Device," Chapter in Book: *Thermoelectr. Power Generation - A Look at Trends in the Technology*, IntechOpen, London, UK, 2016.

[31] K. Pietrzyk, J. Soares, B. Ohara, and H. Lee, "Power generation modeling for a wearable thermoelectric energy harvester with practical limitations," *Appl. Energy*, vol. 183, pp. 218–228, 2016.

[32] M. Gomez, B. Ohara, R. Reid, and H. Lee, "Investigation of the Effect of Electrical Current Variance on Thermoelectric Energy Harvesting," vol. 43, no. 6, pp. 1744–1751, 2014.

[33] H. Oon, C. Houng, S. Sarah, S. Parasuraman, and M. K. A. A. Khan, "Energy Harvesting From Human Locomotion: Gait Analysis, Design and state of art," vol. 42, pp. 327–335, 2014.

[34] Shashank Priya · Daniel J. Inman, *Energy Harvesting Technologies*. Springer US, 2009.

[35] F. Geben, "Modeling and Simulation of Solar Energy Harvesting Systems with Artificial Neural Networks," MS Thesis, Mid-Sweden University, 2016.

[36] Eaton PB Supercapacitors, Eaton, Fareham, England, 2017.

[37] F. M. Jansen, G. H. Van Kollenburg, C. B. M. Kamphuis, F. H. Pierik, and D. F. Ettema, "Hour-by-hour physical activity patterns of adults aged 45-65 years: A cross-sectional study," *J. Public Heal. (United Kingdom)*, vol. 40, no. 4, pp. 787–796, 2018.

[38] A. F. B. F. P. Denilson de Castro Teixeira, Nidia Aparecida Hernandes, Vanessa Suziane Probst, Ercy Maria Cipulo Ramos, "Profile of physical activity in daily life in physically independent elderly men and women," pp. 645–655, 2012.

[39] B. Maamer, A. Boughamoura, A. M. R. Fath El-Bab, L. A. Francis, and F. Tounsi, "A review on design improvements and techniques for mechanical energy harvesting using piezoelectric and electromagnetic schemes," *Energy Convers. Manag.*, vol. 199, no. February, p. 111973, 2019.

[40] P. Howden-Chapman, L. Signal, and J. Crane, "Housing and Health in Older People: Ageing in Place," *Soc. Policy J. New Zeal.*, vol. 13, pp. 14–30, Jan 1999.

[41] J. Saraswat and P. P. Bhattacharya, "Effect of Duty Cycle on Energy Consumption in Wireless Sensor Networks," *Int. J. Comput. Networks Commun.*, vol. 5, no. 1, pp. 125–140, 2013.

Molly Sharone (M'21) received her B.S. in Electrical and Electronics Engineering in 2018 and M.S. in Sustainable Environment and Energy Systems (SEES) in 2021 both from Middle East Technical University Northern Cyprus Campus (Mersin, Turkey). She currently works with UNEP/CTCN, as a Climate Technology Specialist working on technology transfer and implementation for mitigation and adaptation to climate change.

Ali Muhtaroglu (SM'04) received the B.S. in Electrical Engineering from University of Rochester, NY, USA, the M.S. in Electrical and Computer Engineering from Cornell University, NY, USA, in 1996, and the PhD in Electrical and Computer Engineering from Oregon State University in 2007. He worked on multiple commercial microprocessors and mobile computer technologies at Intel Corporation, California and Oregon, USA between 1996-2007. He is currently a faculty member in the Department of Mechanical, Electronic and Chemical Engineering (MEK), and a member of Advanced Health Intelligence and Brain-Inspired Technologies (ADEPT) research group at OsloMet. His background includes mixed signal circuits, energy harvesting circuits and systems, and energy efficient system architectures.